JAMECH
Vol. 46, No. 1, January 2015, pp 13- 19

Numerical Simulation of Nugget Geometry and Temperature Distribution in Resistance Spot Welding

M. Hamedi [1*] and H. Eisazadeh [2]

1. Associate Professor, School of Mechanical Engineering, University of Tehran, Tehran, Iran

2. MS Graduate, School of Mechanical Engineering, University of Tehran, Tehran, Iran

Received 8 June 2014; Accepted 24 July 2014

Abstract

Resistance spot welding is an important manufacturing process in the automotive industry for assembling bodies. The quality and strength of the welds and, by extension, the body is mainly defined by the quality of the weld nuggets. The most effective parameters in this process are sheet material, geometry of electrodes, electrode force, current intensity, welding time and sheet thickness. The present research examined the effect of process parameters on nugget formation. A mechanical/ electrical/ thermal coupled model was created in a finite element analysis environment. The effect of welding time and current, electrode force, contact resistivity and sheet thickness was simulated to investigate the effect of these parameters on temperature of the faying surface. The physical properties of the material were defined as nonlinear and temperature dependent. The shape and size of the weld nuggets were computed and compared with experimental results from published articles. The proposed methodology allows prediction of the quality and shape of the weld nuggets as process parameters are varied. It can assist in adjusting welding parameters that eliminates the need for costly experimentation. This process can be economically optimized to manufacture quality automotive bodies.

Keywords: *nugget size, resistance spot welding, thermo-electro-mechanical analysis.*

1. Introduction

Resistance spot welding (RSW) is commonly used in the automotive industry to join thin sheets of metal. This method is faster and more easily automated and maintained than arc welding. RSW is a complex process that requires interaction of electrical, thermal, mechanical and metallurgical phenomena. In this process, the materials to be joined are brought together under pressure using a pair of electrodes and a high electric current is passed between the electrodes through the work pieces. The contact resistance and joule heating form a molten weld nugget between the work pieces, which are joined as solidification of the weld pool occurs.

* Corresponding Author, Tel.: +98 21 88003318
Email: mhamedi@ut.ac.ir

Force is applied before, during and after the application of electric current, to maintain continuity of the electric current and provide the pressure necessary to form the weld nugget. The total heat generated between two sheets per unit time is defined as the product of the square of the current intensity multiplied by the total resistance and welding efficiency. There is a direct correlation between heat generation and nugget size in RSW. Contact resistance at the faying surface between the work pieces, current density, welding time and sheet thickness mainly determine heat generation during welding and nugget size.

The quality and strength of the welds are affected by the shape and size of weld nuggets and weld quality is usually stated in terms of weld nugget diameter. The relationship between nugget size and welding quality is specified in the handbook of the Resistance Welder Manufacturers' Association. The present study examined nugget formation and the effect of process parameters on the shape and size of the weld nuggets. The effect of RSW parameters was simulated using the finite element method (FEM) to increase the size of the nugget diameter. A mechanical/electrical/thermal coupled model was simulated in a FEM environment using commercially available software. The effect of welding time and current, electrode force, contact resistivity and sheet thickness on the temperature of the faying surface was investigated. The shape and size of the weld nuggets were computed and compared with experimental results from published articles.

2. Literature Review

Many researchers have examined the use of RSW to increase the strength of products using experimental and numerical techniques [1-14]. Experimental studies on nugget formation [1-5,7] have provided valuable temperature data, but the test techniques have limitations and require expensive equipment. Industry is seeking ways to decrease the expense of testing and numerical simulation [6-14] is an attractive alternative to experimental methods. RSW has been studied using one-dimensional (1D), two-dimensional (2D) and, occasionally, three-dimensional (3D) models.

Greenwood [1-2] was the first researcher to use the finite difference method for modeling RSW. They assumed the material properties to be constant and that temperature and heat were not lost from the free surfaces. The joule heat from the interface was calculated using electrical measurements. Nied [6] examined RSW using FEM to analyze the effect of the geometry of an electrode on the work piece and to predict the deformation and stresses as a function of temperature. Their model was limited to elastic deformation and did not calculate the contact areas between the electrode, sheet and faying surface.

Gould [7] measured nugget growth using metallographic techniques and proposed a finite difference-based 1D heat transfer model. This model demonstrated how radial heat transfer inhibits the calculation of nugget expansion, but it did not account for non-uniform current density distribution. In 1D models, heat flow is restricted to the axial direction (z-axis) and cannot account for heat loss into the surrounding sheet (r-axis). Gould's model is not appropriate to simulate nugget growth in thicker sheets.

Tsai [8-9] created a 2D symmetric model using ANSYS to perform parametric studies on spot welding. Khan [10] developed a model to predict nugget development during RSW of Al alloys. The model calculated time by varying interface pressure and only determined the effect of electrode shape and applied pressure on nugget growth. Feulvarch [13] used FEM for electrothermal coupling and general formulation of electrothermal contact conditions between electrodes and sheets. A comparison of their numerical results and thermo-metallurgical experimental measurements showed that the calculated nugget appeared earlier. It was also observed that the nugget grew faster across the thickness.

Hou [14] developed and analyzed a 2D axisymmetric thermo/elastic/plastic FEM using ANSYS. They investigate the behavior of the mechanical features during RSW and determined the distribution and change in contact pressure at the electrode-work piece interface and on the faying surface. They also determined the stress and strain distribution and deformation of the weld, and the displacement of the electrode.

3. Theoretical Analysis

3.1. Governing equation

All equations in this study are based on the 2D cylindrical coordinate system. The governing equation for calculation of the heat generation per unit volume is:

$$q = \frac{1}{R}[\nabla\Phi]^2 \quad (1)$$

where q is heat generated per unit, R is electrical resistivity and ϕ is the electrical potential. The governing equation for transient temperature field distribution, which involves electrical resistance heat, is:

$$\frac{1}{r}\frac{\partial}{\partial r}\left(r\alpha\frac{\partial T}{\partial r}\right)+\frac{1}{r}\frac{\partial}{\partial z}\left(r\alpha\frac{\partial T}{\partial z}\right)+q=\rho c\frac{\partial T}{\partial t} \quad (2)$$

where r and z are the radial and axial coordinates, respectively, ρ is density, c is specific heat, and K is thermal conductivity. The equation calculates the rate of internal heat generation per unit of volume within the boundary of the region of analysis. This term includes the Joule heating caused by bulk resistivity in the sheet-electrode system.

Since thermal/ elastic/ plastic behavior is highly nonlinear, the stress-strain relation is described in incremental form as:

$$\{\Delta\sigma\}=[D]\{\Delta\varepsilon\}+\{C\}\Delta T \quad (3)$$

where vectors $\Delta\sigma$ and $\Delta\varepsilon$ are the stress and strain increment, respectively, and ΔT is temperature increment. Matrix D and vector C are material-related constants.

3.2. Boundary conditions

In all numerical models, the boundary conditions and material properties must be accurate to obtain realistic results. Figure 1 shows the electrical thermal and mechanical boundary conditions used in the model. A 60 Hz sine wave electrical current flow was uniformly distributed along the top surface of the upper electrode and was permitted to flow across the contact areas at the electrode-work piece and work piece-work piece interfaces to reach the bottom surface of the lower electrode. The reference electrical potential bottom of the lower electrode was set to zero. To simulate the effect of cooling water in the electrode cavity, the temperature of the electrode-water interface was maintained at a constant value during welding. A 4670 N mechanical load was applied as a pressure condition at the nodes on the top face of the upper electrode. It was increased linearly during the squeeze time and was held constant during the welding and holding times. Radial displacement was restricted along the r-axis. To simplify analysis, sliding at the electrode-sheet interface was not modeled.

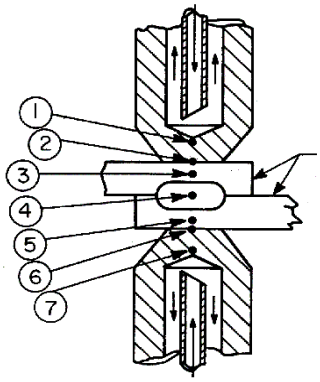

Fig. 1. Schematics of resistance spot welding

3.3. Material properties

The steel sheets used were of AISI 1008 steel composed of 0.08 C, 0.32 Mn and 0.018 S and the electrodes were copper. The temperature-dependent physical and mechanical properties of materials that were used for electro-thermal and thermal-mechanical analysis were thermal conductivity, coefficient of thermal expansion, electrical resistance, specific heat, density, enthalpy, elasticity of yield stress and Poisson's ratio.

3.4. Welding conditions

Welding comprised four cycles: squeezing, welding, holding and cooling. The exact welding constants used in this study are given in Table 1.

Table 1. Welding constants used in this study

Welding current	Welding time	Electrode force	Electrode diameter	Electrode taper	Sheet Thickness
14.2 KA	14 cycles	4670 N	7.6 mm	30 deg	1.52 mm

4. Numerical Technique

RSW was treated as an electrical/ thermal/mechanical problem to be solved using FEM. The commercial finite element code ANSYS was used to model coupling between electrical and thermal phenomena and between the thermal and mechanical phenomena. The nodal temperature distribution and updating of deformed geometrical information is done using APDL language. Temperature-dependent thermal, electrical and mechanical properties of the material, including contact resistance, were considered. Because the nature of the electrode and the work pieces is symmetric, a split physical model for 2D analysis is shown in Figure 2.

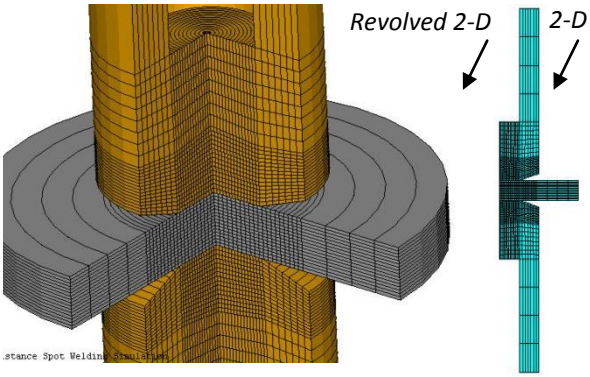

Fig. 2. FEM model for resistance spot welding

5. Results and Discussion

5.1. Spot nugget growth

FEM was employed to simulate RSW to quantitatively determine the effects of the process parameters on temperature distribution and nugget size in the different cycles. Nugget formation during RSW was predicted for the squeeze, welding and holding time and was then compared with experimental data from Gould et al. [7].

5.1.1. Welding time

Figures 4 and 5 show the temperature profile and nugget growth for the eighth and fourteenth cycles of welding, respectively. The results are displayed on a half model obtained during post-processing. The melting point of AISI 1008 steel was assumed to be 1530°C; this is the point at which the spot nugget region turns red. The highest temperature was always found at the middle of the work piece. The temperature profile was varied by changing the boundary conditions, which in turn changed the nugget size and welding quality.

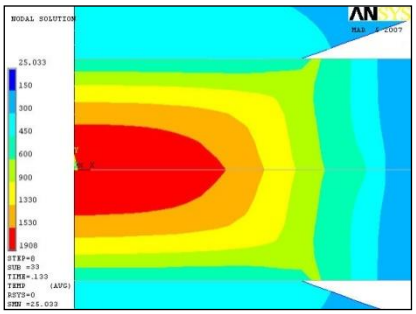

Fig. 4. Temperature distribution at 8th cycle of welding

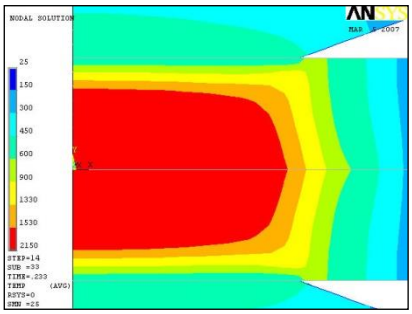

Fig. 5. Temperature distribution at 14th cycle of welding

During simulation, the weld nugget began to form in the fifth weld cycle and it quickly grew in the lateral and vertical directions over the next 2-3 cycles. Growth slowed after about three cycles when about 60% of the thickness of the work piece was achieved, because of contact resistance ceased in response to the high temperature. The highest temperature in the weld nugget was always observed to be in the middle of the faying surface. This indicates that contact resistance plays a critical role in the duration of the first weld cycle.

5.1.2. Holding and cooling time

In the thermo-mechanical model during the holding cycle, the current is set to zero and the convection and squeezing forces are external loads. The final nugget size is obtained at the end of cooling time because some deformation in the welding zone occurs when the weld cools in response to electrode pressure and material shrinkage.

The results of RSW from the FEM were compared with the experimental results from

Gould et al. [7]. To maintain consistency, the dimensions of the work piece, material properties, welding conditions and boundary conditions used were the same as in Gould et al. [7]. A comparison between the shapes of the weld nugget from Gould et al. and the results of FEM at a welding current of 14200 A and a welding time of 14 cycles is shown in Figure 6. The thickness of the experimental molten zone was about 2.12 mm and the calculated thickness was 2.23 mm. It indicates a good agreement between the calculated results and the experimental data.

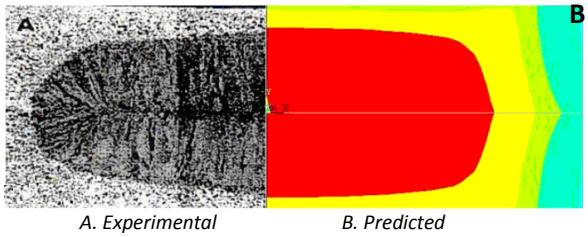

Fig. 6. Schematic of predicted and experimental weld nugget cross-section dimensions

5.2. Effect of welding parameters

Weld quality is stated in terms of weld nugget diameter. The present study observed the effect on nugget dimension and geometry of welding current, welding time, electrode force, contact resistance and sheet thickness. Previous studies have considered other parameters. For example, electrode force was studied by Khan [10], but the more realistic and advanced FEM model used in the present study allows adjustment of welding parameters for to optimum nugget dimensions.

5.2.1. Effect of welding current on nugget size

Welding current has the greatest effect on generation of heat at the faying surface, thus, it is a primary control variable in RSW. Figure 7 shows the influence of welding current on nugget dimensions. The weld nugget formed at a welding current higher than 14.5 kA, indicating that welding current has a strong influence on the weld nugget at currents of 15.5–16.2 kA. The experimental data and 1D model developed by Gould et al. [7] are shown for comparison and indicate that the results from the FEM agree well with the experimental data.

5.2.2. Effect of welding time on nugget size

Figure 8 shows the influence of welding time on weld dimensions in RSW. Experimental data and results of the 1D model [7] are presented for comparison. Nugget growth predicted by FEM agrees well with the experimental data and the 1D model predicts realistic shapes of curves. The 1D model curves differed from the calculated results. Gould suggested that these discrepancies can be attributed to either radial conduction in the sheet or inaccurate characterization of faying surface resistance. The calculated results indicate that the weld nugget commenced during cycle 8 in the welding time and increased abruptly after 6 cycles. The rate of increase of weld nugget thickness decreased with the increase in weld time.

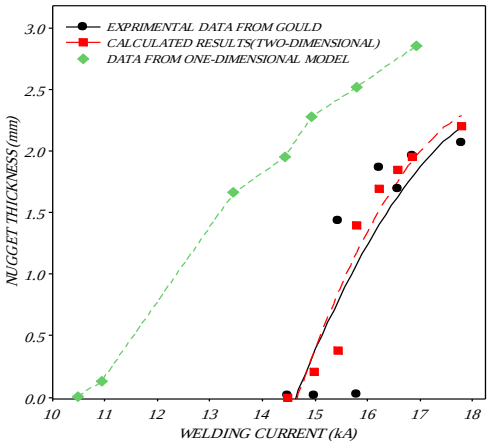

Fig. 7. FEM vs. experimental data from Gould et al. [7] with 1.52 mm sheets, 6 weld cycles at 4760 N

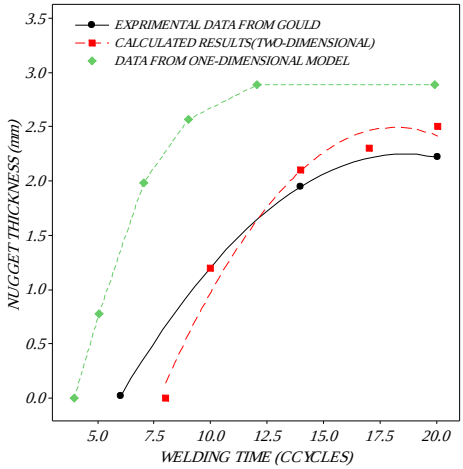

Fig. 8. FEM vs. experimental data from Gould et al. [7] with 1.52 mm sheets at 13 kA and 4760-N

5.2.3. Effect of contact resistance and electrode force on nugget size and shape

The results of simulations illustrate the effect of contact resistance on the faying surface. The results shown in Figure 9 indicate that contact resistance is a critical factor in RSW of steel followed by electrode force. Faying contact resistance in the Joule equation is influenced by this factor.

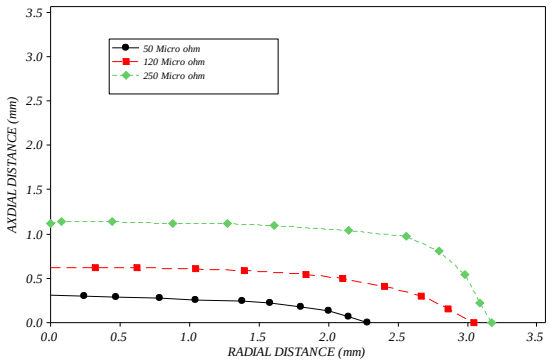

Fig. 9. Nugget formation vs. contact resistance

Electrode force helps keep the weld intact until it solidifies, cools and the weld nugget reaches maximum strength. To examine the effect of electrode force on nugget size, the contact area and the temperature distributions were calculated using different electrode forces. Table 2 summarizes the predicted contact areas at three load levels. A correlation was observed between the loads at 4670 and 6500 N.

Table 2. Welding conditions used in this study

Electrode Force	4670N	5500N	6500N
Contact Area	4.66mm	4.78mm	4.9mm

Figure 10 shows the nugget size at load level 3 and illustrates an indirect correlation between electrode force and nugget size. As the electrode force increased, the time to reach the melting temperature increased because of the decrease in total resistance. The decrease in total resistance is to be expected when the increase in applied pressure decreased the current density in response to the increase in contact area. Expulsion occurred with a decrease or elimination in load level to increase nugget size. A suitable level of electrode force must be selected and integrated to prevent expulsion.

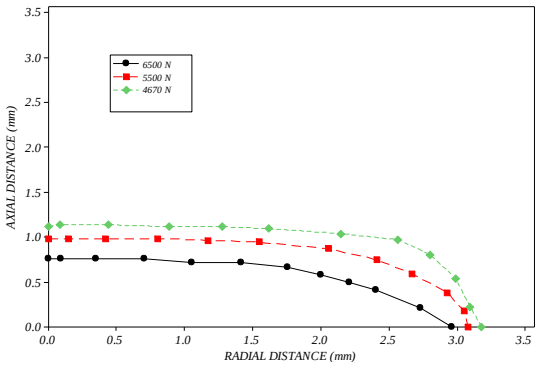

Fig. 10. Nugget formation vs. welding force

6. Conclusions

The present study used an incremental and thermal/electro/mechanical coupled FEM to predict the temperature distribution and spot nugget size in a spot-welded steel joint. Simulations were performed for coupled analysis for different stages of the welding cycle by providing the necessary information and boundary conditions. Experimental data and a 1D model from Gould et al. [7] were used for comparison. The results provide information about the development of the weld nugget to help predict weld quality without requiring actual test welding. The input parameters can be adjusted to provide weld nuggets of different sizes. Optimum settings for the welding parameters for specific quality levels and materials of the work piece can be obtained by simulation without performing a large amount of testing.

The following conclusions can be drawn from this study:

- If the electrical current exceeds the flow necessary for nugget growth, it causes a rapid growth of the nugget. The nugget growth rate decreased as the current flow increased, but the nugget size increased until melt spattering occurred.
- Increasing the number of electrical cycles strongly increased the contact surface temperature; this caused melting of the contact zone and produces a large nugget without melt spattering. An increase in weld time gives equilibrium to the melt pool.
- Increasing the load on the electrodes decreased the nugget size and increased the contact surface area.

- When plate thickness increased, the current needed for the formation of a weld nugget increased. Decreasing the plate thickness decreased the diameter of the electrode.

Refrences

[1].Bentley K.P., Greenwood J. A., McK Knowlson P., 1963, Temperature distribution in spot welding, British Welding Journal **12**: 613-619.

[2].Greenwood J. A., 1963, Temperature in spot welding, British Welding Journal **6**: 316-322.

[3].Nagel Lee, Nagel G. L., 1988, Basic phenomena in resistance spot welding, Society of Automotive Engineers Technical Paper. No. 880277.

[4].Cho H. S., Cho Y. J., 1989, A study of the thermal behavior in resistance spot welds, Welding Journal **68**: 236s-244s.

[5].Kim E., Eager T. W., 1988, Transient thermal behavior in resistance spot welding, sheet metal, in: Welding Conference III, Detroit, MI.

[6].Nied H. A., 1984, The finite element modeling of the resistance spot welding process, Welding Journal **63**(4): 123.

[7].Gould J. E., 1994, An examination of nugget development during spot welding using both experimental and analytical techniques, Welding Journal **66**(1): 1-10.

[8].Tsai C. L., Jammal O. A., Dickinson D. W., 1992, Modeling of resistance spot weld nugget growth, Welding Journal **71**(2): 47s-54s.

[9].Tsai C. L., Jammal O. A., Dickinson D. W., 1989, Study of nugget formation in resistance spot welding using finite element method, Paper presented at the trends in welding research, in: 2nd International Conference. Materials Park, OH., USA.

[10]. Khan J.A., Xu L., Chao Y., Broach K., 2000, Numerical simulation of resistance spot welding process, Numerical Heat Transfer, Part A **37**: 425–446.

[11]. Richard D., Fafard M., Lacroix R., Clery P., Maltais Y., 2003, Carbon to cast iron electrical contact resistance constitutive model for finite element analysis, J. Mater. Process. Technol. **132**: 119–131.

[12]. Chang B. H., Zhou Y., 2003, Numerical study on the effect of electrode force in small-scale resistance spot welding, J. Mater. Process. Technol. **139** (1–3): 635–641.

[13]. Feulvarch E., Robin V., Bergheau J.M., 2004, Resistance spot welding simulation: a general finite element formulation of electrothermal contact conditions, J. Mater. Process. Technol. **153–154**: 436–441.

[14]. Hou Z., Kim I., 2007, Finite element analysis for the mechanical features of resistance spot welding process, J. Mater. Process. Technol. **180**: 160-165.